Supporting Information

Quantum Plasmonics: Optical Monitoring of DNA-Mediated Charge Transfer in Plasmon Rulers

*Sarah Lerch and Björn M. Reinhard**

Experimental Methods

DNA Programmed Self-Assembly of PRs.

A1: Citrate stabilized gold NPs were mixed with a fully complementary 5'–thiolated DNA handles (Integrated DNA Technologies, IDT) in a ratio of 1:5,000 (NP:DNA) in ~50 µL. AT and CG rich sequences were used: AT-Seq1 (HS-AAA TTG ATC TTA AAG TTG TTC AAC TAC CTA AAA AAG TTA A), AT-Seq2 (HS-ACT TTT TTA GGT AGT TGA ACA ACT TTA AGA TCA ATT T), GC-Seq1 (HS-GGG ACG TGG CGT GGT GGA GCT GGC TGG AGG GCG CGT GCC G), GC-Seq2 (HS-CGG CAC GCG CCC TCC AGC CAG CTC CAC CAC GCC ACG TCC C). The NaCl concentration in the DNA / NP mixes was gradually raised from 0 mM to ~400 mM through multiple small additions of NaCl over a 36 hour period. The formed NP-DNA conjugates were then washed by repeated centrifugation and resuspension (5x in T20 – 20mM NaCl, 10mM Tris-HCl, pH 7.0; 1x in T80). Equal volumes of the NP conjugates were combined and incubated for 2 minutes before the addition of a non-thiolated version of Seq1. After 15 minutes of incubation, a non-thiolated version of Seq2 was added. The hybridization mix was then purified on a 1% agarose gel, using a 0.5x Tris Borate EDTA (TBE) running buffer at 140V for 30 minutes. The dimer band was isolated from the gel and the dimers were recovered through electroelution and stored in 60mM Tris buffer at 4° C for up to 3 days.

A2: Citrate stabilized NPs was incubated with Bis(p-sulfonatophenyl)phenylphospine (BSPP,0.6g/mL) for 16 hours. The BSPP-stabilized nanoparticles were then incubated with Seq1 in a 1:1 ratio in T20 for 12 hours. After that, an excess of short DNA was added, AT-Seq1-short (HS-TTT TTT TTT TTT TTT TTT TT) or CG-Seq1-short (HS-GG GCG GGC GGG CGG GCG GGC), and incubated for another 12 hours. Following the 24 hour DNA incubation period, the NaCl concentration of the solution was raised from 20 mM to ~400 mM through multiple small additions of NaCl over a 36 hour period. A second batch of NP DNA conjugates was prepared with the corresponding Seq2 as described under *S1*. The nanoparticle-DNA conjugates were washed by repeated centrifugation and resuspension (5x in T20, 1x in T80). Equal volumes of the nanoparticle conjugates (50 μL, 5 x 10^9 particles/mL) were then combined and incubated overnight before the addition of the non-thiolated versions of Seq1 and Seq1-short, to suppress the formation of larger clusters. The mixture of monomers, dimers and larger clusters was purified by gel-electrophoresis as described for *S1*.

TEM Sample Preparation. A carbon Type-B three slot grid (Ted Pella, Inc) was used for the correlative darkfield spectroscopy and TEM analysis. These grids were incubated with polylysine solution (10 μL, 2%) for 10 minutes in a water vapor saturated environment. A drop of PRs solution was incubated on the grid for 10-30 s before it was removed with the help of a filter paper. The grid was then incubated with 10 μL of 2.0μm polystyrene (PS) marker beads (0.04%, Thermo Scientific Duke Standards). Finally, the grid was rinsed with T60 and DDI water. Grids were dried under ambient atmosphere for 30 minutes and then stored under vacuum for up to 1 week before optical analysis in the darkfield microscope.

Darkfield Measurements and Spectrum Processing. Optical measurements were performed with an Olympus BX51WI microscope under darkfield illumination (numerical aperture, NA = 1.2-1.4) using unpolarized whitelight from a 100W Tungsten lamp. The scattered light was collected with a 60x oil objective (NA = 0.65) and either imaged with a back-illuminated

CCD camera (Andor DV437-BV) or spectroscopically analyzed using a 303 nm focal length imaging spectrometer (Andor, Shamrock) with a 150 lines/mm grating and back-illuminated CCD camera (Andor DU401-BR-DD). The recorded spectra were background corrected by subtracting the spectrum of an area void of PRs and corrected for the spectral profile of the excitation light. Once the grid was fully analyzed, the glycerol was removed through a quick rinse in methanol, followed by a rinse in DDI water. The glycerol immersion and methanol wash do no affect on the PRs, as seen in **Figure S1**.

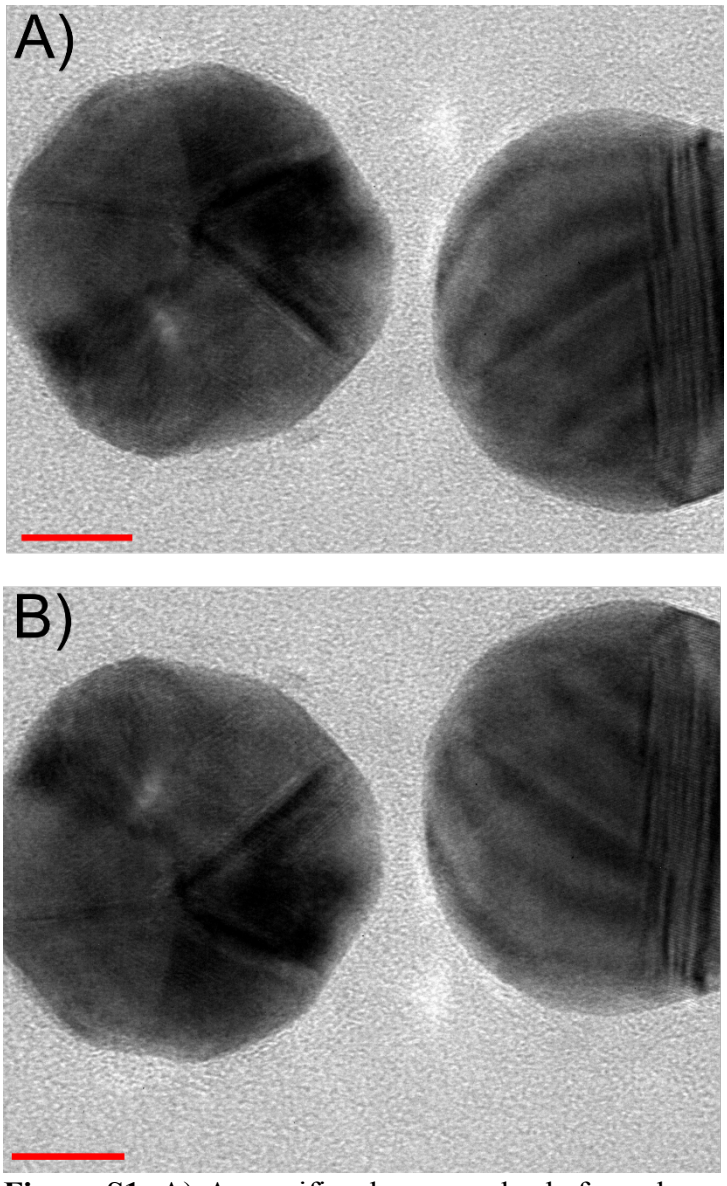

Figure S1. A) A specific plasmon ruler before glycerol immersion and methanol wash. B) The same plasmon ruler (rotated 180° during TEM sample loading phase) after glycerol immersion for 2 hours and methanol washing procedure described in text.

TEM Imaging. Correlated TEM measurements were obtained as described in the main text on an FEI Tecnai Osiris TEM at 200 kV. Initial low magnification images were taken from 60x to 1800x while higher magnifications used were 120kx, 180kx, and 255kx. Due to the morphology changes induced by the electron beam in the TEM, some of the images show a darkening, particularly in the short separation gaps. This darkening is an artifact of the TEM which does not influence the spectra, since they are obtained prior to the TEM imaging, as noted in the main text.

Plasma Cleaning and Hyperspectral Analysis. Plasma cleaning samples were prepared by incubating polylysine (2%, 100 μL) on a cleaned glass slide for 15 minutes. After washing with DDI water, Au PRs (*A1* synthesis, 100 μL, ~ 6 x 10^9 NPs/mL) were incubated on the slide for 30 seconds. After a final DDI wash, the sample was dried and observed on an Inverted darkfield microscope (Olympus IX71, NA = 0.92-0.8) using unpolarized light from a 100W Tungsten lamp. Scattered light was collected using a 60x air objective (NA = 0.1 – 1.3) and imaged using a back-illuminated CCD (Andor iXon+). After initial white light investigation of the sample, the area of interest was then imaged using a multispectral filter (CRi Varispec) from 500 nm to 700 nm, every 20 nm. Following the analysis with no plasma cleaning, the sample was subjected to O_2 plasma (Harrick Plasma, 10W) for 15 seconds. Further darkfield and multispectral imaging was completed for the same area of interest. This process was completed for time points at 0, 15, 30, 45, 60 seconds. A further experiment with long (80 base pairs) DNA: AT-Seq1 (HS-TTT TTT TTT ATT TTT TTT TAT TTT TTT TTA TTT TTT TTT ATT TTT TTT TAT TTT TTT TTA TTT TTT TTT ATT TTT TTT TT), AT-Seq2 (HS-AAA AAA AAA ATA AAA AAA AAT AAA AAA AAA TAA AAA AAA ATA AAA AAA AAT AAA AAA AAA TAA AAA AAA ATA AAA AAA AA), synthesized using the *A2* synthesis and procedure above, were performed to demostrate that the observed red-shift is an effect of the DNA only in short separations. Spectra from long DNA were analyzed and the $\Delta\lambda_{res}$ versus the initial λ_{res} for each PR is shown in **Figure S2.** As noted in

the main text, there is a clear sub-population with $\lambda_{res} < 570$ nm which displays a significant red-shift upon plasma cleaning. This population explains the small red-shift observed during the long DNA experiment. A control sample of DNA-conjugated 80 nm Au NPs was analyzed in the same fashion for 0 and 120 seconds to determine that the plasma cleaning itself did not contribute to the effect observed and the distributions are presented in **Figure S3**.

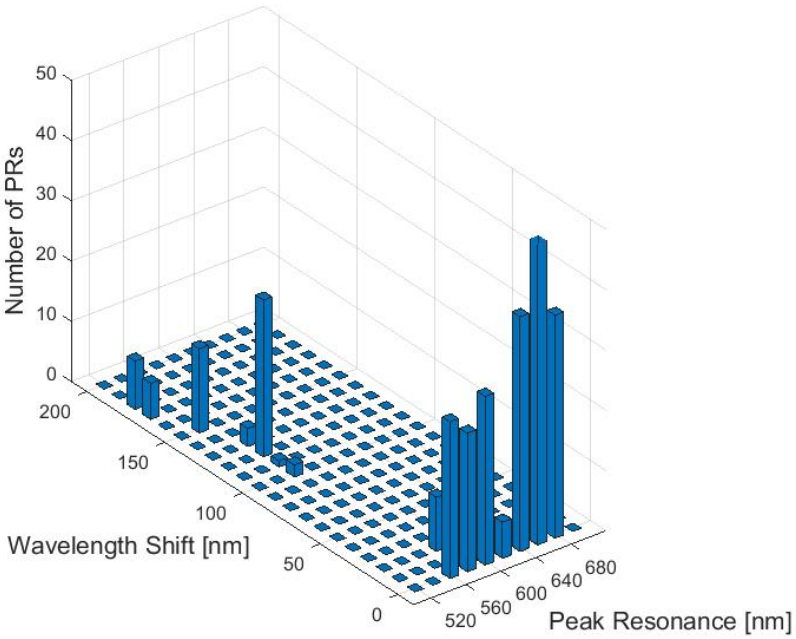

Figure S2. Distribution of long DNA PRs with regards to the peak resonance wavelength (nm) and the $\Delta\lambda_{res}$ (nm). The distribution demonstrates two distinct populations, those with initial resonances below 570 nm (which have a large red-shift after plasma cleaning) and those with longer peaks resonances (which do not demonstrate the red-shift after plasma cleaning).

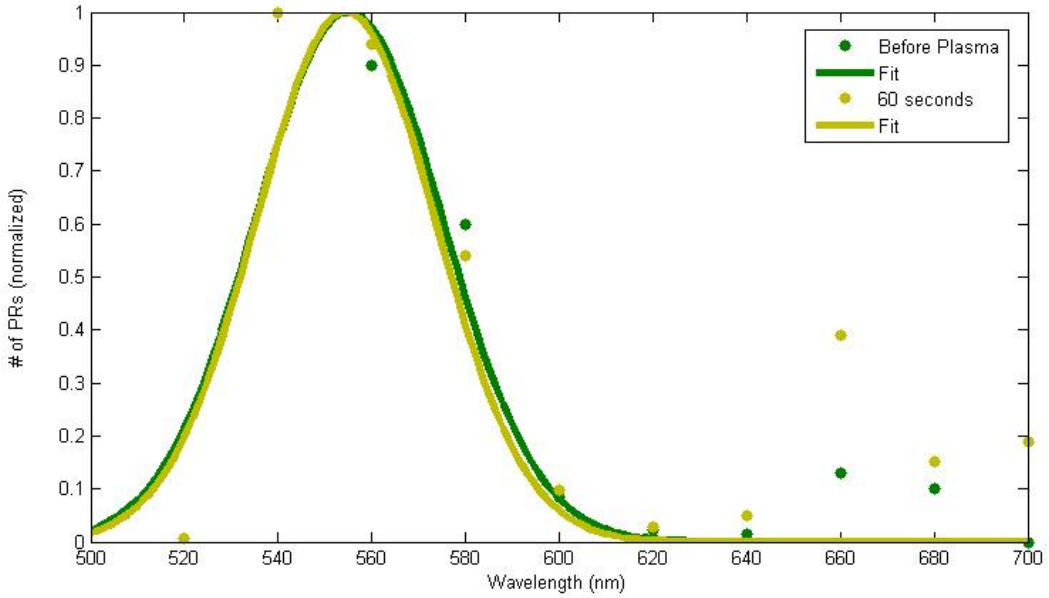

Figure S3. Number of NPs vs. peak λ_{res} for the control DNA-conjugated 80nm Au NPs before (green) and after (yellow) plasma cleaning for 120 seconds.

Simulation Set-Up. FDTD simulations for dimers of 40 nm gold NPs were performed using Lumerical FDTD solutions (version 8.7) using the Johnson and Christy dielectric functions for gold[1] and assuming an ambient refractive index of $n_r = 1.57$. The simulation area was a cube defined with 400 nm length on each side and a cubic mesh override region of 140 nm^3 with a 2 nm mesh size. A further mesh override area with a 0.25nm mesh size was created directly around the gap of the nanoparticles (center-to-center) to ensure accurate information about the conductive junction area. A total field scattered field source was injected 120 nm below the plane of the dimers, with a wavelength range of 300 to 2000 nm and a polarization parallel to the dimer axis. The scattered light was detected by six 2-D power detectors on each side of the mesh override region. The permittivity of the gap region was defined as described in the text. The conductivities used in the determination of the gap region are mentioned in the main text as $\sigma_0 = 7.8$ S/m for the charge transfer regime ($S < 3$nm) or $\sigma_0 = 0.6$ S/m for the charge hopping regime ($S > 3$ nm). These values are the the result of averaging values

obtained for AT and CG sequences,[2] which do not exhibit enough difference to change the resonance spectra and resulting $\Delta\lambda/\lambda_0$ vs. *S/D* curve (**Figure S4**). We also note that our conductivities neglected the transverse direction for the individual bases.[3] While this direction shows a signficantly larger difference between individual bases, the PRs that involve this range ($S < 1$ nm) will have junction areas (A) that encompass a variety of bases, making the differences between the sequences negligible.

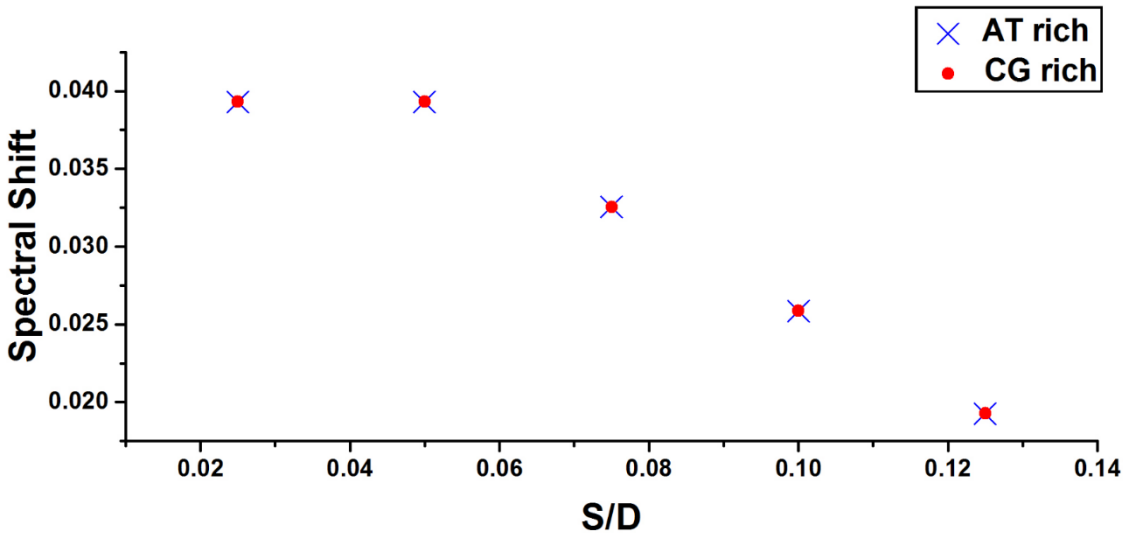

Figure S4. $\Delta\lambda/\lambda_0$ vs. *S/D* curve for AT rich conductivity (σ_0 = 6.6 S/m) vs. CG rich conductivity (σ_0 = 9.2 S/m), indicating that the difference in the conductivities from S = 1 nm to S = 5 nm (*S/D* = 0.025:0.125) is not noticeable in the plasmon resonance, as observed in the main text.

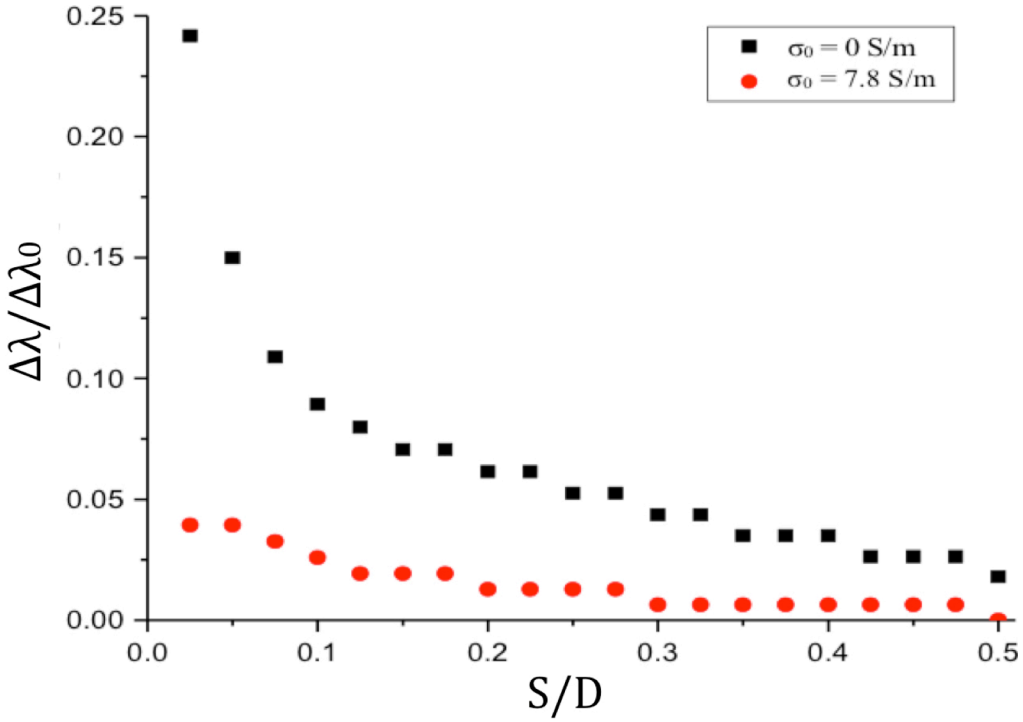

Figure S5. Simulated spectral shifts as a function of separation (*S/D*) for σ_0 = 7.8 S/m (red) and σ_0 = 0 (black).

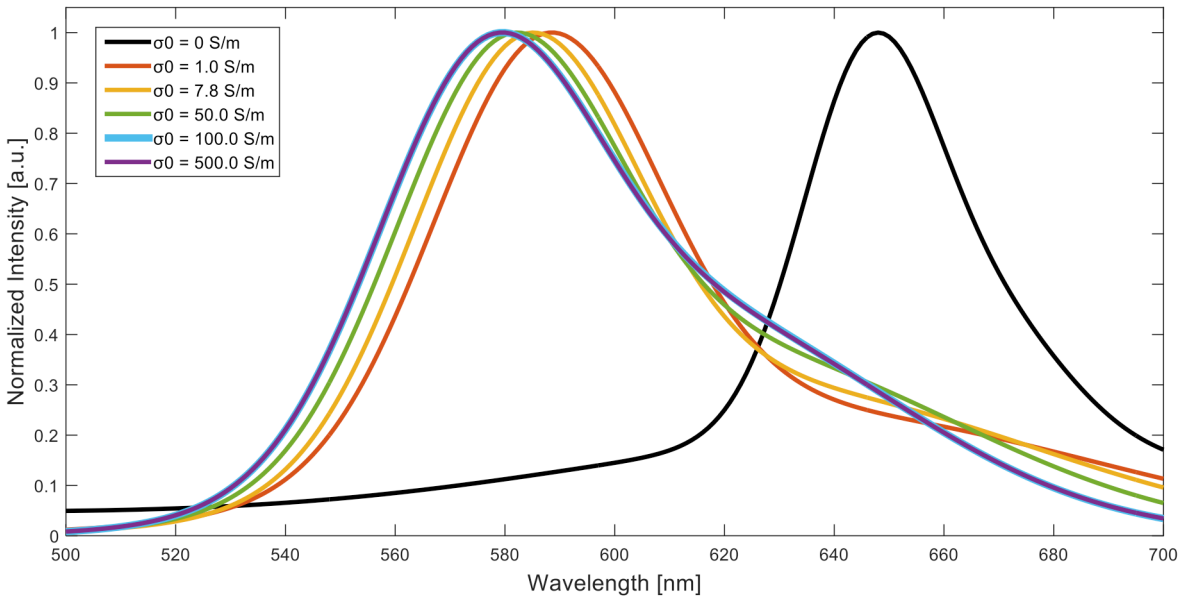

Figure S6. Simulations for σ_0 = 0 S/m (black), 1.0 S/m (red), 7.8 S/m (orange), 50.0 S/m (green), 100.0 S/m (blue), and 500.0 S/m (purple) a one fixed separation (*S* = 2 nm) demonstrate the effect of increasing conductivity on the spectra at short interparticle separations.

[1] P. B. Johnson, R. W. Christy, *Physical Review B* **1972**, *6*, 4370.

[2] D. Dulic, S. Tuukkanen, C-L. Chung, A. Isambert, P. Lavie, A. Filoramo, *Nanotechnology* **2009**, *20,* 115502.

[3] a) J. He, L. Lin, P. Zhang, Q. Spadola, Z. Xi, Q. Fu, S. Lindsay, *Nano Lett.* **2008**, *8*, 2530; b) M. Zwolak, M. Di Ventra, *Nano Lett.* **2005**, *5*, 421.